Geophysical Research Letters

RESEARCH LETTER
10.1029/2018GL077429

Independent DEM of Antarctica Using GNSS-R Data From TechDemoSat-1

Jessica Cartwright[1,2], **Maria Paola Clarizia**[3,4], **Paolo Cipollini**[1,5], **Christopher J. Banks**[6], **and Meric Srokosz**[1]

[1]National Oceanography Centre, Southampton, UK, [2]Ocean and Earth Science, National Oceanography Centre Southampton, University of Southampton, Southampton, UK, [3]Geography and Environment, University of Southampton, Southampton, UK, [4]Now at Deimos Space UK, Harwell Oxford, UK, [5]Telespazio VEGA UK Ltd. for European Space Agency/ECSAT, Harwell, UK, [6]National Oceanography Centre, Liverpool, UK

Key Points:
- Altimetry over glacial ice from satellite GNSS-Reflectometry is presented for the first time over the extent of the Antarctic continent
- Elevation of the ice is estimated from GNSS-R data from the TechDemoSat-1 satellite
- Good agreement is observed with CryoSat-2 1-km DEM v1.0

Supporting Information:
- Supporting Information S1

Correspondence to:
J. Cartwright,
jc1n15@noc.soton.ac.uk

Citation:
Cartwright, J., Clarizia, M. P., Cipollini, P., Banks, C. J., & Srokosz, M. (2018). Independent DEM of Antarctica using GNSS-R data from TechDemoSat-1. *Geophysical Research Letters*, *45*, 6117–6123. https://doi.org/10.1029/2018GL077429

Received 1 FEB 2018
Accepted 29 MAY 2018
Accepted article online 11 JUN 2018
Published online 21 JUN 2018

Abstract The first digital elevation model (DEM) of the Antarctic ice sheet derived from Global Navigation Satellite Systems-Reflectometry (GNSS-R) data from the UK TechDemoSat-1 satellite is presented. This is obtained using 32 months of data from the mission. This opportunistic and inexpensive method is shown to produce encouraging results from the technology demonstration platform of TechDemoSat-1, with median bias under 18 m and root-mean-square difference under 91 m when compared to the CryoSat-2 1-km DEM v1.0. Discrepancies between the two data sets are explored along with possible causes of such differences and potential improvements to further optimize this technique for future GNSS-R missions.

Plain Language Summary Obtaining measurements of the Antarctic ice sheet is critical for understanding the effects that climate change might be having on it and its potential future contribution to rising sea levels. The only practical way to do this is by using satellite data, and this has been done successfully previously from the CryoSat-2 satellite, which carries a radar altimeter. However, due to its orbit, it cannot measure an area near the South Pole. Here we demonstrate that measurements of the Antarctic ice sheet, including the vicinity of the South Pole, can be made by taking advantage of GPS signals that bounce off the ice sheet surface. The data are obtained from the UK's TechDemoSat-1 mission, which carries a simple low-cost receiver to pick up the reflected GPS signals. The results from this demonstration mission (which was not designed to survey ice sheets) are promising, showing the potential of this approach for measuring the ice sheet in the future with a dedicated satellite mission.

1. Introduction and Rationale

Global Navigation Satellite Systems-Reflectometry (GNSS-R) was first proposed in 1988 (Hall & Cordey, 1988) and uses reflected L-band radiation from GNSS signals such as those of Global Positioning System (GPS) to characterize the Earth's surface. At present this is predominantly used for monitoring winds (Clarizia & Ruf, 2016; Foti et al., 2015, 2017) and sea state (Marchan-Hernandez et al., 2010). It is also being explored extensively for other Earth observation purposes such as soil moisture detection (Masters et al., 2000), sea surface height (Clarizia et al., 2016) and sea ice monitoring (Belmonte-Rivas et al., 2010; Gleason, 2006). Specific cryospheric applications of GNSS-R include the detection of sea ice (Alonso-Arroyo et al., 2017; Yan & Huang, 2016), ice sheet altimetry (Rius et al., 2017), and altimetry of sea ice through both the delay of the reflected echo (Hu et al., 2017) and its carrier phase delay (Li et al., 2017). The use of GNSS-R for altimetry purposes was first proposed by Martín-Neira through a passive reflectometry and interferometry system (Martín-Neira, 1993), and has been very successful over a wide range of studies including fixed, airborne, and space-borne experiments. Initial airborne precisions measured include 3 m over the sea (Ruffini et al., 2004) and up to 5 cm over inland water bodies (Lowe, 2002). Recently accuracies of 10–90 cm have been attained (Semmling et al., 2013), and as such it can be seen as a very promising technique for the altimetry field. Due to the specular nature of reflections from ice and the necessity of satellite techniques to monitor these areas, it is a natural step to apply these methods to land-based ice sheets. As noted by Slater et al. (2018), accurate DEMs can contribute to the delineation of drainage basins, the estimation of grounding line ice thickness, mass balance calculations, boundary conditions for models of ice dynamics, and potential sea level rise.

L-band signals were first shown to be sensitive to submeter ice elevation changes in 2004 (Cardellach et al., 2004), but this level of accuracy depends on using the phase delay of a coherent signal (Li et al., 2017) that is not applicable when the scattering is more diffuse. More recently, GNSS-R signals have been proven to distinguish ocean, transition zone, and glacial ice (Rius et al., 2017). In their study, Rius et al. (2017) identified factors affecting the reflected signal and this study builds on that through the application of an algorithm previously used to measure sea surface height (Clarizia et al., 2016). This algorithm is applied over the extent of the Antarctic ice sheet using all available data from the Low-Earth Orbiter TechDemoSat-1 (TDS-1) and compared primarily with a Digital Elevation Model (DEM) from the European Space Agency's CryoSat-2 (Slater et al., 2018), as it is the most recent of the Antarctic DEM releases. Two earlier DEMs (Bamber et al., 2009; Fretwell et al., 2013) independent of the CryoSat-2 data are also used for a comparison.

This paper presents elevation estimates of the Antarctic ice sheet, the first application of GNSS-R to obtain a DEM of Antarctica, by applying Clariza et al.'s (2016) algorithm to TDS-1 data. Section 2 discusses the data used and the satellite platform; section 3 summarizes the methods used and results. Validation of the results against the CryoSat-2 1-km DEM v1.0 (Slater et al., 2018) and other independent data sets is performed in section 4, as well as discussing the necessary further investigations to improve the accuracy of this technique. The conclusions of the study are given in section 5.

2. TDS-1 and GNSS-R—Data

Data from GNSS-R sensors are provided in the form of delay-Doppler maps (DDMs). A DDM can be seen as a map of the scattered power in the delay and Doppler domains. A smooth reflecting surface produces a strong, coherent reflection in GNSS-R. This means that the scattered power comes almost entirely from the specular point and the glistening zone is very small. The corresponding DDMs will have a pronounced peak and a limited spreading of the power distribution. Ice is considered smooth compared to the sea surface at the scale of GPS L-band wavelength (19 cm), giving particularly strong reflections in the DDMs and making them ideal for the extraction of height information, though land ice may give more diffuse reflections than sea ice. A strength of GNSS-R for applications such as these lies in the receipt of reflections from up to four different GPS satellites at any one time by the receiver. This, in addition to the asynchronism of the TDS-1 cycle with that of the GPS satellites, allows a varying web of specular points to be built up over time and therefore a high spatial resolution to be attained, as well as access to some points such as the poles, which due to necessary satellite inclination, have thus far not been possible to measure using satellite altimetry. However, this does introduce difficulties into the verification of measurements made at the highest latitudes, due to lack of independent validation data.

TDS-1 was designed as a satellite technology demonstration platform by Surrey Satellite Systems Ltd., carrying eight experimental payloads, of which one was the Space GNSS Receiver Remote Sensing Instrument (SGR-ReSI) from which the data in this study were obtained. This instrument is extremely low-power and low-mass and is constructed from commercial components. Full details can be found in Jales and Unwin (2015). TDS-1 was placed into a quasi-sun-synchronous orbit of 98.4° inclination at an altitude of 635 km. Due to the use of a shared platform, the SGR-ReSI was active 2 days in an 8-day cycle. These data are provided as 1-s DDMs and metadata in 6-hr windows in a publicly accessible database (merrbys.co.uk). Each DDM is made up of 128 delay pixels by 20 Doppler pixels, with a resolution of 0.252 chips (0.246 μs) and 500 Hz respectively. The vertical resolution that results from this depends largely on the geometries of the satellites at the time (Cardellach et al., 2014).

The data used in this study have been taken from 3 years of service from TDS-1 (November 2014 to July 2017) with specular points south of 60°S and filtered in order to eliminate noise. This has been achieved by excluding points where the power distribution of the DDM is less coherent than a normal distribution using the kurtosis of the DDM. DDMs with a kurtosis much greater than 3 (the value for a Gaussian distribution) display a clear signal. The threshold for discarding DDMs was fixed to be a kurtosis of 3.5. This threshold was chosen so as to ensure the removal of all noisy points below the threshold and to account for the uncertainty in the noise estimation. Increasing the threshold to 4 made little difference to the results, and therefore, the lower threshold was used in order to return more data. Further points were removed according to quality flags provided with the data.

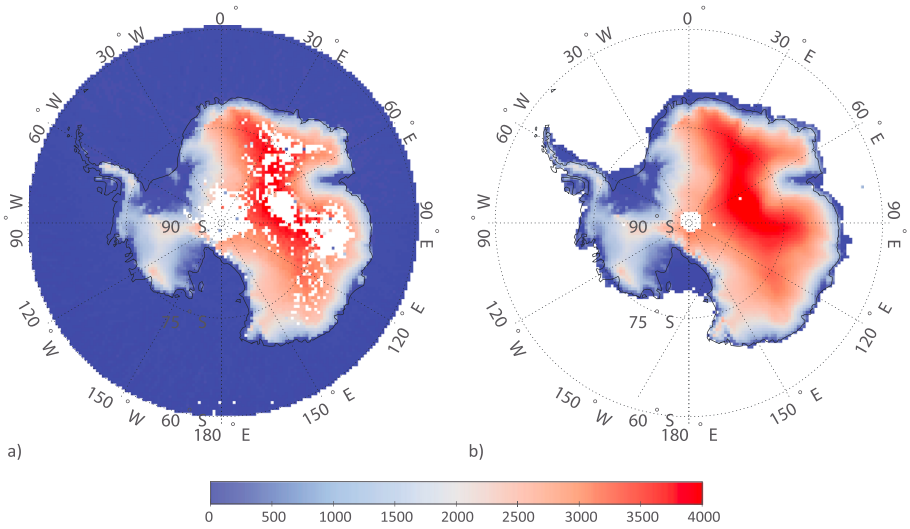

Figure 1. Digital elevation models from (a) TechDemoSat-1 data and (b) CryoSat-2 (Slater et al., 2018). Elevations are shown in meters above the ellipsoid with white denoting no available data.

Being a technology demonstration mission, the sensor on board TDS-1 is not optimized for altimetric applications. As such, the tracking window for received signals is tied to the ellipsoid, which causes loss of signal where high elevations such as those of the Antarctic ice sheet are concerned. These data points have been identified by the maximum amplitude of the DDM straying from the central four Doppler bins of the DDM (as the central peak is out of the tracking window). These have been filtered out where the Doppler value at the maximum amplitude (dop_{ma}) is outside the range:

$$\frac{dop_{min}}{10} < dop_{ma} < \frac{dop_{max}}{10} \tag{1}$$

where dop_{min} is the minimum of the Doppler axis and dop_{max} the maximum. These criteria were chosen as they remove all data points where the signal has left the tracking window and prevents saturation at the top of the tracking window (often above about 2,400-m elevation). Further data omitted are those where the maximum amplitude is in the first delay row of the DDM, as no leading edge is visible in the waveform. Data that are flagged as containing the direct signal in the DDM are removed due to disruption of the tracking of the reflected signal, and those in Collection Period 12 (September 2016) are also filtered due to changes in the DDM processor settings that made these DDMs inconsistent.

The data used include both modes of gain control, as the power of the signal itself is not used in the height estimation. Contrary to previous studies, samples were not filtered by antenna gain, but an incidence angle filter was applied to remove points where reflections were at an incidence angle of 55° or greater. The data collected at larger angles were seen to overestimate heights by up to 200 m near the pole. The inclusion of these data yields an almost gap-free DEM, though this is not presented in this paper due to the largely unconstrained overestimations. The extended DEM and comparisons with CryoSat-2 data are provided in the supporting information.

The most recent release (May 2018) of the CryoSat-2 DEM (Slater et al., 2018) is used as a comparison to ensure the highest accuracy of control variable for comparison.

3. GNSS-R Altimetry of Antarctic Continental Ice—Methods and Results

The elevation algorithm of Clarizia et al. (2016) uses the locations of both the transmitter and receiver satellites from the TDS-1 metadata to estimate height through the time delay between the expected receipt of the signal (were it to reflect off the ellipsoid) and the actual time of receipt. The geometry then allows the calculation of the reflective surface above the ellipsoid. In order to extract this delay from the TDS-1 DDMs, the maximum power is tracked in the Doppler domain to identify the waveform as it varies in delay space (the column of the DDM that corresponds to the maximum power). The sampling is increased in the delay domain through Fourier transform interpolation of this waveform, at an interpolation factor of 1,000

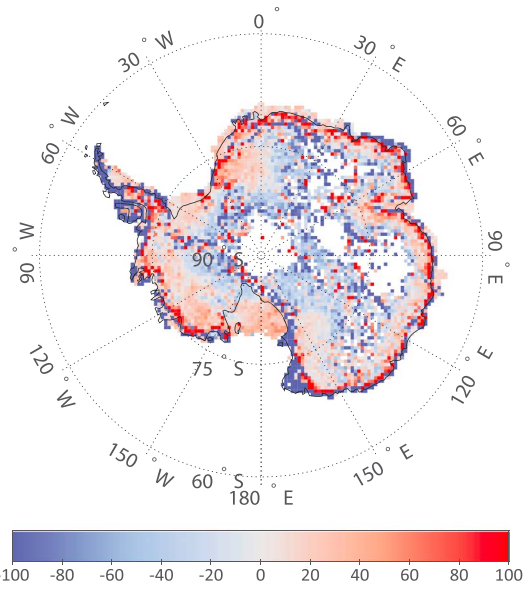

Figure 2. Comparison of TechDemoSat-1 heights in meters over Antarctica and those from CryoSat-2 data (Slater et al., 2018). (TechDemoSat-1 minus CryoSat-2).

(Clarizia et al., 2016) before the maximum first-order derivative of the leading edge is identified. This interpolation method is used in order to preserve the spectrum in the frequency domain throughout the interpolation process and has been seen to reduce the errors. The method to identify the leading edge derivative follows the process outlined in Hajj and Zuffada (2003), whereby the first-order derivative is calculated for the leading edge of the waveform and the maximum of this is used to represent the delay between the direct and reflected signal. This delay value is then used for elevation calculations based on the geometry of the bistatic arrangement (as found in Clarizia et al., 2016). Details of the measurement geometry and delay estimation can be found in the supporting information, as can a discussion of tracking maximum power instead of the leading edge to obtain height estimates.

After filtering, a significant number of samples were found to have values less than zero relative to the ellipsoid and were simply discarded. The remaining data are averaged over a 50 × 50 km grid for comparison to the CryoSat-2 DEM 1 km v1.0 (Slater et al., 2018) as reference. For these comparisons, the CryoSat-2 DEM was filtered for negative samples and gridded in the same manner to ensure comparability of measurements (Figures 1 and 2). This resolution was chosen so as to maximize both coverage and accuracy of the final product. Varying this resolution between 20 and 100 km gave no obvious improvement to the results (see the supporting information). For calculation of root-mean-square and median differences quoted below, colocated ungridded data were used through linear interpolation of the CryoSat-2 DEM to the locations of the TDS-1 specular points. This gives the noisier appearance seen in the CryoSat-2 data in Figure 3.

4. Comparison With CryoSat-2 Data—Discussion

The DEM presented in Figure 1 suggests that the use of GNSS-R for altimetry over land ice is feasible and increases the potential for height measurements over the pole, which is currently not estimated with any existing satellite (see the supporting information). The comparison of this with the CryoSat-2 DEM 1 km v1.0 (Figures 2 and 3) gives an insight into the accuracy of this technique, yielding a median error of 17.9 m and an RMS error of 90.7 m over the extent of the ice sheet. This error is fairly consistent with other available DEMs for comparison, as detailed in Table 1. The slope of the ice surface, derived from the CryoSat-2 DEM, results in changes in the error with a median and RMS error, respectively, of 13.8 and 68.1 m for slopes below 0.25° to 37.9 and 96.8 m for slopes between 0.75° and 1°. Further error estimates due to the slope of the ice surface and comparisons with the Bedmap2 and Bamber et al.'s (2009) DEMs can be found in the supporting information.

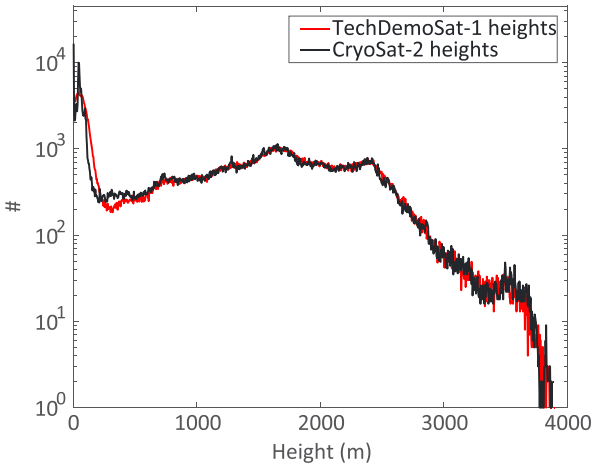

Figure 3. Histogram of colocated height data over Antarctica from CryoSat-2 (black; Slater et al., 2018) and TechDemoSat-1 (red).

Rius et al. (2017) in their study of Greenland along two tracks quote 8.5 m as the "expected uncertainty in the delay measurements," but this is not an actual error estimate obtained by comparing GNSS-R measurements with independent observations. More comparable are the results of Slater et al. (2018), Griggs and Bamber (2009), and Fretwell et al. (2013) who quote overall RMS errors of 13.5, 5.0, and 30.0 m, respectively, for their Antarctic DEMs. However, in areas where the DEM has been interpolated, Slater et al. (2018) state that there are median and RMS differences of 19.62 and 117.77 m, respectively, as compared to airborne data. The latter figures are not dissimilar to the ones obtained here.

Due to the nature of the platform as a demonstrator and the operating cycle of the SGR-ReSi, the DEM (Figure 1) is not complete, with many holes resulting from areas without suitable data within the period of TDS-1 data used here. Where data acquired at higher incidence angles are included, the majority of these gaps disappear, but some points are overestimated (see the supporting information). The density plot (Figure 4) also displays

Table 1
Comparison With Other Available DEMs

DEM	Reference	Median difference (m)	RMS difference (m)
CryoSat-2 1 km	Slater et al. (2018)	17.9445	90.6924
ERS-1 and ICESat	Bamber et al. (2009)	18.7009	79.8821
Bedmap2 Surface DEM	Fretwell et al. (2013)	19.2476	83.0065

Note. Bamber et al. (2009) and Bedmap2 (Fretwell et al., 2013) are independent from the CryoSat-2 DEM, the former based on data from ERS-1 and ICESat, and the latter a compilation of many DEMs (including that of Bamber et al., 2009). The DEMs used in this comparison all use kriging or other interpolation technique and where this has been used to fill in the area around the pole where there is no data those estimates have been omitted from this comparison. DEM = digital elevation model; RMS = root-mean-square.

a large number of points underestimated at around the origin within the TDS-1 data set in relation to CryoSat-2. These correspond to data retrieved from the edge of the ice shelf (values of −100 m in Figure 2) and may be due to corner effects giving multiple DDM peaks or misplaced specular points.

Known issues in the TDS-1 data set are covered in detail in Clarizia et al. (2016) and include uncertainty of the satellite attitude and orbit (and thus the specular point), as well as experimental changes in settings given its use as a technology demonstration platform. Attitude is provided by both the sun sensors and the magnetometers, with the latter in use when the satellite is in eclipse. The uncertainty in the magnetometer readings is larger than those of the sun sensors (up to 10°; Foti et al., 2017). Sudden large corrections can also occur when switching between the two sensors, though no correlation has been seen between these changes and error patterns seen here. One important change in the sensor settings through the mission is that of the switch from Automatic Gain Mode to Fixed Gain Mode (April 2015), resulting in a change in the absolute power seen in the DDM. This is also affected by antenna effects, which (despite much progress; Gleason et al., 2016; Voronovich & Zavorotny, 2018) are not yet definitively quantified for this sensor. A strength of this elevation estimation algorithm is that the absolute power of the DDM cells is not considered, making it possible to use data from both modes without calibration of the two or normalization of the DDMs.

A large unknown in L-band altimetry is the penetration depth of the signal into materials such as snow and ice. This can vary in magnitude from tens of centimeters to hundreds of meters (Li et al., 2017; Mätzler, 2001) and is due to the large range of physical properties of these materials with changing densities and precipitation regime. For example, Rignot et al. (2001) measured penetration depths of 3 to 120 m over the Greenland ice sheet, depending on the terrain. A further consideration is the atmospheric uncertainties associated with the ionosphere and troposphere above the polar ice cap. These are largely unknown at these high latitudes but are thought to be much smaller than our magnitude of error (maximum of 10 m at the equator; Mainul & Jakowski, 2012).

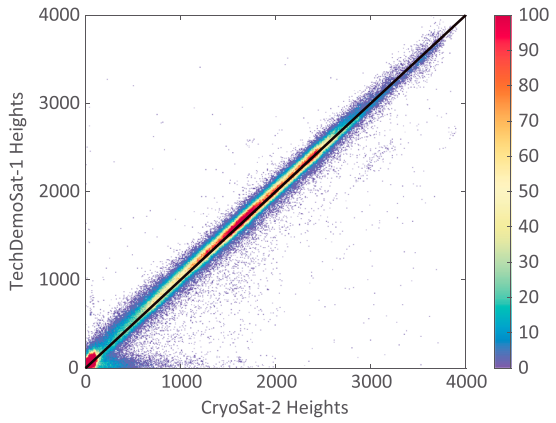

Figure 4. Density plot comparing height estimations from TechDemoSat-1 over Antarctica and colocated data from CryoSat-2 DEM (Slater et al., 2018) with 1:1 reference line (black). DEM = digital elevation model.

Errors are also associated with the averaging period used for both the TDS-1 data and that of the CryoSat-2 DEM. Due to the temporal extent involved in the calculations, smaller-scale effects such as seasonality were explored but no correlation was found with discrepancies from the CryoSat-2 DEM. As such, these seasonal effects and their associated changes in penetration depth have been ignored.

5. Conclusions

We have demonstrated through this study that altimetry of land ice is possible with GNSS-R to an accuracy of approximately 18 m, if CryoSat-2 is taken as truth. This is the first time that GNSS-R has been used to create an independent DEM over land ice and has potential significance as data collected covers the pole area, which until now was not possible to map with satellite altimetry.

The use of the technology demonstration platform to produce these results reveal great potential for the future of this technique, as further increases in accuracy and understanding may be achieved using a sensor

and platform optimized for such measurements. In future studies it will be necessary to understand and mitigate errors such as those causing the overestimation of points at high incidence angles. This will enable this technique to produce a full DEM of the Antarctic ice sheet with improved accuracy and coverage, including the South Pole. It will also be necessary to optimize any platform and sensor for such measurements and to improve processing strategies, such as centering the delay-Doppler window around the true specular point on the Earth surface to ensure all data are received within the tracking window. In order to improve the estimation of the surface elevation, modelling of the signal scattering and penetration through the ice will be necessary, with the objective of quantifying the penetration depth under different conditions, and its variations due to seasons and climate.

Owing to the reliance of the technique on signals of opportunity and the lightweight nature of the receiver, the harnessing of this technology for the monitoring of the cryosphere would provide an inexpensive yet highly effective solution. The recent launch of the CYGNSS constellation in 2016 for the application of GNSS-R to tropical wind measurements brings up the possibility of a polar mission of a similar format. Reflections over ice are much more coherent and therefore stronger than those over oceans. The application of this technology to such a mission would therefore provide much higher spatiotemporal resolution of measurements in polar regions (average 4-hr revisit time for CYGNSS satellites; Ruf et al., 2013), allowing improved monitoring of all aspects of this dynamic system, including sea-ice interactions (which have not been considered here). To determine the feasibility of such a mission would require a careful consideration of the error budget to determine the accuracy of the height measurements possible, but this is beyond the scope of this paper. In addition, further improvements to measurement accuracy may be possible using interferometric techniques (Martín-Neira et al., 2011) or phase delay information (Cardellach et al., 2004; Li et al., 2017), but the latter depends on having a coherent return from the surface.

In terms of the future applications of GNSS-R to monitoring the Antarctic ice sheet, it may be possible to deduce properties of Antarctic snow and ice by combining these observations with those from passive L-band instruments, such as SMOS (e.g., Macelloni et al., 2016), and at other microwave frequencies, such as K_u-band from CryoSat-2.

Acknowledgments
The authors are grateful to the TechDemoSat-1 team at SSTL for making all collection data publicly available (www.merrbys.co.uk). Thanks are also due to the providers of all DEMs used in our comparison for making them available publicly. This is found for CryoSat-2 1-km DEM v1.0 at http://www.cpom.ucl.ac.uk/csopr/icesheets2/dems.html; that of Bamber et al. (2009) at http://nsidc.org/data/NSIDC-0422; and the Bedmap2 DEM at https://www.bas.ac.uk/project/bedmap-2. The authors would also like to thank the anonymous reviewers who helped improve this manuscript. This work was supported by the Natural Environmental Research Council (grant NE/L002531/1). The DEM created in this study is available at https://doi.org/10.5285/2ef1c932-1fd2-4593-a793-f37815ab6f82.

References

Alonso-Arroyo, A., Zavorotny, V. U., & Camps, A. (2017). Sea ice detection using U.K. TDS-1 GNSS-r data. *IEEE Transactions on Geoscience and Remote Sensing*, *55*(9), 4989–5001. https://doi.org/10.1109/TGRS.2017.2699122

Bamber, J. L., Gomez-Dans, J. L., & Griggs, J. A. (2009). A new 1 km digital elevation model of the Antarctic derived from combined satellite radar and laser data Part 1: Data and methods. *Cryosphere*, *3*(1), 101–111. https://doi.org/10.5194/tc-3-101-2009

Belmonte-Rivas, M., Maslanik, J. A., & Axelrad, P. (2010). Bistatic scattering of GPS signals off arctic sea ice. *IEEE Transactions on Geoscience and Remote Sensing*, *48*(3 PART2), 1548–1553. https://doi.org/10.1109/TGRS.2009.2029342

Cardellach, E., Ao, C. O., de la Torre Juárez, M., & Hajj, G. A. (2004). Carrier phase delay altimetry with GPS-reflection/occultation interferometry from low Earth orbiters. *Geophysical Research Letters*, *31*, L10402. https://doi.org/10.1029/2004GL019775

Cardellach, E., Rius, A., Martin-Neira, M., Fabra, F., Nogues-Correig, O., Ribo, S., et al. (2014). Consolidating the precision of interferometric GNSS-r ocean altimetry using airborne experimental data. *IEEE Transactions on Geoscience and Remote Sensing*, *52*(8), 4992–5004. https://doi.org/10.1109/TGRS.2013.2286257

Clarizia, M. P., & Ruf, C. S. (2016). Wind speed retrieval algorithm for the cyclone global navigation satellite system (CYGNSS) mission. *IEEE Transactions on Geoscience and Remote Sensing*, *54*(8), 4419–4432. https://doi.org/10.1109/TGRS.2016.2541343

Clarizia, M. P., Ruf, C., Cipollini, P., & Zuffada, C. (2016). First spaceborne observation of sea surface height using GPS Reflectometry. *Geophysical Research Letters*, *43*, 767–774. https://doi.org/10.1002/2015GL066624

Foti, G., Gommenginger, C., Jales, P., Unwin, M., Shaw, A., Robertson, C., & Roselló, J. (2015). Spaceborne GNSS reflectometry for ocean winds: First results from the UK TechDemoSat-1 mission. *Geophysical Research Letters*, *42*, 5435–5441. https://doi.org/10.1002/2015GL064204

Foti, G., Gommenginger, C., Unwin, M., Jales, P., Tye, J., & Rosello, J. (2017). An assessment of non-geophysical effects in spaceborne GNSS reflectometry data from the UK TechDemoSat-1 mission. *IEEE Journal of Selected Topics in Applied Earth Observations and Remote Sensing*, *10*(7), 3418–3429. https://doi.org/10.1109/JSTARS.2017.2674305

Fretwell, P., Pritchard, H. D., Vaughan, D. G., Bamber, J. L., Barrand, N. E., Bell, R., et al. (2013). Bedmap2: Improved ice bed, surface and thickness datasets for Antarctica. *Cryosphere*, *7*(1), 375–393.

Gleason, S. (2006). Remote sensing of ocean, ice and land surfaces using bistatically scattered GNSS signals from low earth orbit (PhD thesis). IEEE, Islamabad, Pakistan. https://doi.org/10.1109/ICASE.2015.7489519

Gleason, S., Ruf, C. S., Clarizia, M. P., & O'Brien, A. J. (2016). Calibration and unwrapping of the normalized scattering cross section for the cyclone global navigation satellite system. *IEEE Transactions on Geoscience and Remote Sensing*, *54*(5), 2495–2509. https://doi.org/10.1109/tgrs.2015.2502245

Griggs, J. A., & Bamber, J. L. (2009). A new 1 km digital elevation model of Antarctica derived from combined radar and laser data-Part 2: Validation and error estimates. *Cryosphere*, *3*(1), 113–123.

Hajj, G. A., & Zuffada, C. (2003). Theoretical description of a bistatic system for ocean altimetry using the GPS signal. *Radio Science*, *38*(5), 1089. https://doi.org/10.1029/2002RS002787

Hall, C., & Cordey, R. (1988). Multistatic scatterometry, International Geoscience and Remote Sensing Symposium. *Remote Sensing: Moving Toward the 21st Century*, *1*, 561–562. https://doi.org/10.1109/IGARSS.1988.570200

Hu, C., Benson, C., Rizos, C., & Qiao, L. (2017). Single-pass sub-meter space-based GNSS-R ice altimetry: Results from TDS-1. *IEEE Journal of Selected Topics in Applied Earth Observations and Remote Sensing*, *10*(8), 3782–3788. https://doi.org/10.1109/JSTARS.2017.2690917

Jales, P., & Unwin, M. (2015). Mission description-GNSS reflectometry on TDS-1 with the SGR-reSI (Tech. Rep. SSTL Rep, 248367). Guildford, UK: Surrey Satellite Technol. Ltd.

Li, W., Cardellach, E., Fabra, F., Rius, A., Ribó, S., & Martín-Neira, M. (2017). First spaceborne phase altimetry over sea ice using TechDemoSat-1 GNSS-R signals. *Geophysical Research Letters*, *44*, 8369–8376. https://doi.org/10.1002/2017GL074513

Lowe, S. T. (2002). 5-cm-Precision aircraft ocean altimetry using GPS reflections. *Geophysical Research Letters*, *29*(10), 1375. https://doi.org/10.1029/2002GL014759

Macelloni, G., Leduc-Leballeur, M., Brogioni, M., Ritz, C., & Picard, G. (2016). Analyzing and modeling the SMOS spatial variations in the East Antarctic Plateau. *Remote Sensing Applications*, *180*, 193–204. https://doi.org/10.1016/j.rse.2016.02.037

Mainul, M., & Jakowski, N. (2012). Ionospheric propagation effects on GNSS signals and new correction approaches. *Global Navigation Satellite Systems: Signal, Theory and Applications* (pp. 381–404). Neustrelitz: InTech. https://doi.org/10.5772/30090

Marchan-Hernandez, J. F., Valencia, E., Rodriguez-Alvarez, N., Ramos-Perez, I., Bosch-Lluis, X., Camps, A., et al. (2010). Sea-state determination using GNSS-R data. *IEEE Geoscience and Remote Sensing Letters*, *7*(4), 621–625. https://doi.org/10.1109/LGRS.2010.2043213

Martín-Neira, M. (1993). A passive reflectometry and interferometry system (PARIS): Application to ocean altimetry. *ESA journal*, *17*(4), 331–355.

Martín-Neira, M., D'Addio, S., Buck, C., Floury, N., & Prieto-Cerdeira, R. (2011). The PARIS ocean altimeter In-Orbit demonstrator. *IEEE Transactions on Geoscience and Remote Sensing*, *49*(6), 2209–2237. https://doi.org/10.1109/TGRS.2010.2092431

Masters, D., Zavorotny, V., Katzberg, S., & Emery, W. (2000). GPS Signal scattering from land for moisture content determination. https://doi.org/10.1109/IGARSS.2000.860346

Mätzler, C. (2001). Applications of SMOS over terrestrial ice and snow. In *3rd SMOS Workshop*. DLR, Oberpfaffenhofen, Germany.

Rignot, E., Echelmeyer, K., & Krabill, W. (2001). Penetration depth of interferometric synthetic-aperture radar signals in snow and ice. *Geophysical Research Letters*, *28*(18), 3501–3504. https://doi.org/10.1029/2000GL012484

Rius, A., Cardellach, E., Fabra, F., Li, W., Ribó, S., & Hernández-Pajares, M. (2017). Feasibility of GNSS-R ice sheet altimetry in Greenland using TDS-1. *Remote Sensing*, *9*(7), 742. https://doi.org/10.3390/rs9070742

Ruf, C., Unwin, M., Dickinson, J., Rose, R., Rose, D., Vincent, M., & Lyons, A. (2013). CYGNSS: Enabling the future of hurricane prediction [Remote sensing satellites]. *IEEE Geoscience and Remote Sensing Magazine*, *1*(2), 52–67. https://doi.org/10.1109/MGRS.2013.2260911

Ruffini, G., Soulat, F., Caparrini, M., Germain, O., & Martín-Neira, M. (2004). The eddy experiment: Accurate GNSS-R ocean altimetry from low altitude aircraft. *Geophysical Research Letters*, *31*, L12306. https://doi.org/10.1029/2004GL019994

Semmling, A. M., Wickert, J., Schön, S., Stosius, R., Markgraf, M., Gerber, T., et al. (2013). A zeppelin experiment to study airborne altimetry using specular Global Navigation Satellite System reflections. *Radio Science*, *48*, 427–440. https://doi.org/10.1002/rds.20049

Slater, T., Shepherd, A., McMillan, M., Muir, A., Gilbert, L., Hogg, A. E., et al. (2018). A new digital elevation model of Antarctica derived from CryoSat-2 altimetry. *Cryosphere*, *12*(4), 1551–1562. https://doi.org/10.5194/tc-12-1551-2018

Voronovich, A. G., & Zavorotny, V. U. (2018). Bistatic radar equation for signals of opportunity revisited. *IEEE Transactions on Geoscience and Remote Sensing*, *56*(4), 1959–1968. https://doi.org/10.1109/TGRS.2017.2771253

Yan, Q., & Huang, W. (2016). Spaceborne GNSS-R sea ice detection using delay-doppler maps: First results from the U.K. TechDemoSat-1 mission. *IEEE Journal of Selected Topics in Applied Earth Observations and Remote Sensing*, *9*(10), 4795–4801. https://doi.org/10.1109/JSTARS.2016.2582690